Connection among classical interatomic potential functions

Teik-Cheng Lim

Faculty of Engineering, Nanoscience and Nanotechnology Initiative, 9 Engineering Drive 1, National University of Singapore, S 117576, Republic of Singapore
E-mail: alan_tc_lim@yahoo.com

The four classical interatomic pair potentials of Lennard-Jones [Proc. Roy. Soc. Lond. A 106 (1924) 463], Morse [Phys. Rev. 34 (1929) 57], Rydberg [Z. Phys. 73, (1931) 376] and Buckingham [Proc. Roy. Soc. Lond. A 168 (1938) 264] have been widely adopted in molecular force fields of computational chemistry softwares and also incorporated into 2-body potential energy description in many-body solid-state physics. This paper demonstrates how mathematical methods such as infinite series expansions can be used to connect parameters across these interatomic potential functions.

1. Introduction

Though the quantum mechanical approach is known to be theoretically rigorous, the importance of empirical interatomic potentials are nevertheless undoubted in view of the latter's practicality. For example, the pair potentials of Lennard-Jones [1]

$$U_{\text{LJ}} = D_{\text{LJ}} \left[\left[\frac{R}{r} \right]^{12} - 2 \left(\frac{R}{r} \right)^6 \right], \tag{1}$$

Morse [2]

$$U_{\text{M}} = D_{\text{M}} \left[\exp\left(-2\alpha(r - R)\right) - 2\exp\left(-\alpha(r - R)\right) \right], \tag{2}$$

Rydberg [3]

$$U_{\text{Ryd}} = -D_{\text{Ryd}} \left[1 + a \left(\frac{r - R}{R} \right) \right] \exp\left(-a \left(\frac{r - R}{R} \right) \right) \tag{3}$$

261

and Buckingham [4]

$$U_{B} = A \exp\left(-Br\right) - \frac{C}{r^6} \tag{4}$$

have been adopted in the 2-body portion of the Pearson-Takai-Halicioglu-Tiller (PTHT) [5], the Biswas-Hamann (BH) [6], the Murrell-Mottram (MM) [7] and the Bauer-Maysenholder-Seeger (BMS) [8] empirical potentials respectively. The later potentials, [5–8] consist of both 2-body and 3-body potential energy for describing many-body condensed matter systems, and have been parametrized for silicon [5–7] and FCC metals (Cu, Ag, Au) [8]. As shown in table 1, the 2-body portion of PTHT and MM adopt the exact version of Lennard-Jones and Rydberg potentials, respectively. However, the 2-body portion of BMS is a generalized version of the Buckingham potential. The generalization is more so for the case of BH's 2-body portion in comparison to the Morse potential. As such, this paper primarily develops a simultaneous relationship among the classical functions of Lennard-Jones, Morse, Rydberg and Buckingham potentials, followed by relationships between the classical pair potentials of Morse and Buckingham with the 2-body portion of BH and BMS, respectively. The present work is a follow-up of previous effort in establishing parametric relationships between interatomic potential functions using mathematical approaches [9–20] (figure 1).

2.   Analysis

To obtain near-equilibrium relationship, let

$$\left(\frac{\partial^n U_{B}}{\partial r^n}\right)_{r=R} = \left(\frac{\partial^n U_{LJ}}{\partial r^n}\right)_{r=R} = \left(\frac{\partial^n U_{M}}{\partial r^n}\right)_{r=R} = \left(\frac{\partial^n U_{Ryd}}{\partial r^n}\right)_{r=R} \tag{5}$$

Table 1
Comparison between classical and 2-body portion of modern empirical potentials.

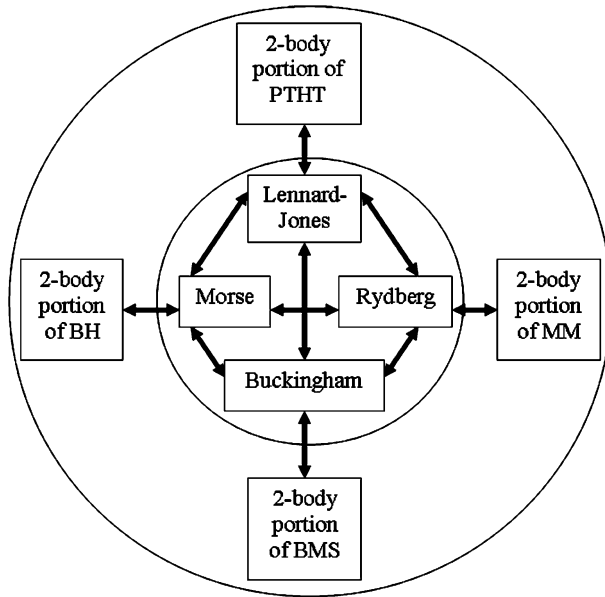| Classical potential functions	2-Body portion of modern potentials
Lennard-Jones [1]	Pearson-Takai-Halicioglu-Tiller [5]
$U_{LJ} = D_{LJ}\left[\left(\frac{R}{r}\right)^{12} - 2\left(\frac{R}{r}\right)^6\right]$	$U_{PTHT} = \varepsilon\left[\left(\frac{R}{r}\right)^{12} - 2\left(\frac{R}{r}\right)^6\right]$
Morse [2]	Biswas-Hamann [6]
$U_{M} = D_{M}\left[\exp\left(-2\alpha(r-R)\right) - 2\exp\left(-\alpha(r-R)\right)\right]$	$U_{BH} = A_1 \exp\left(-\lambda_1 r\right) + A_2 \exp\left(-\lambda_2 r\right)$
Rydberg [3]	Murrell-Mottram [7]
$U_{Ryd} = -D_{Ryd}\left[1 + a\left(\frac{r-R}{R}\right)\right]\exp\left(-a\left(\frac{r-R}{R}\right)\right)$	$U_{MM} = -D_{MM}\left[1 + a\left(\frac{r-R}{R}\right)\right]\exp\left(-a\left(\frac{r-R}{R}\right)\right)$
Buckingham [4]	Bauer-Maysenholder-Seeger [8]
$U_{B} = A \exp\left(-Br\right) - \frac{C}{r^6}$	$U_{BMS} = A \exp\left(-Br\right) - \frac{C}{r^n}$

Figure 1. Simultaneous connection among the classical potential functions (inner circle) as well as with some 2-body portion of modern potentials used in many-body condensed matter systems (outer circle).

for $n = 0, 1, 2$. This results in the following system of equations across the four classical potentials considered herein

$$\begin{bmatrix} \xi^0 & 1 \\ \xi^1 & 6 \\ \xi^2 & 42 \end{bmatrix} \left\{ \begin{array}{c} A \exp(-\xi) \\ -\left(\frac{C}{R^6}\right) \end{array} \right\} = D_{\text{LJ}} \left\{ \begin{array}{c} -1 \\ 0 \\ 72 \end{array} \right\} = D_{\text{M}} \left\{ \begin{array}{c} -1 \\ 0 \\ 2\alpha^2 R^2 \end{array} \right\} = D_{\text{Ryd}} \left\{ \begin{array}{c} -1 \\ 0 \\ a^2 \end{array} \right\}, \quad (6)$$

where the scaling function is defined as

$$\xi = BR. \tag{7}$$

Buckingham's repulsive coefficient, A, can be expressed in terms of its attractive coefficient, C, from the second row of equation (6),

$$\frac{C}{R^6} = \frac{\xi}{6} A \exp(-\xi) \tag{8}$$

which, upon substitution into the first and third rows of equation (6), gives

$$\left(\frac{\xi - 6}{6}\right) A \exp(-\xi) = D_{\text{LJ}} = D_{\text{M}} = D_{\text{Ryd}} \tag{9}$$

and

$$\xi(\xi - 7) A \exp(-\xi) = 72 D_{\text{LJ}} = 2\alpha^2 R^2 D_{\text{M}} = a^2 D_{\text{Ryd}}, \tag{10}$$

respectively. Eliminating the term $A \exp(-\xi)$ from equations (9) and (10) leads to

$$\xi = \begin{cases} \left(\frac{19}{2}\right) \pm \sqrt{\left(\frac{19}{2}\right)^2 - 72} \\ \left(\frac{7}{2} + \frac{\alpha^2 R^2}{6}\right) \pm \sqrt{\left(\frac{7}{2} + \frac{\alpha^2 R^2}{6}\right)^2 - 2\alpha^2 R^2} \\ \left(\frac{7}{2} + \frac{a^2}{12}\right) \pm \sqrt{\left(\frac{7}{2} + \frac{a^2}{12}\right)^2 - a^2} \end{cases} . \tag{11}$$

We note that for any non-negative value of αR or a, the upper and lower solutions for the scaling function are of the range $\xi^{\text{upp}} \geqslant 7$ and $\xi^{\text{low}} \in [0, 6]$, respectively. Since substitution of equations (8) and (9) into equation (4) gives

$$U_{\text{B}} = D \left[\frac{6}{\xi - 6} \exp\left(\xi \left(1 - \frac{r}{R}\right)\right) - \frac{\xi}{\xi - 6} \left(\frac{R}{r}\right)^6 \right], \tag{12}$$

the upper solution of equation (11) is selected to maintain sign consistency between equations (4) and (12). We further note that the first and third rows of equation (6) explicitly show that

$$D_{\text{LJ}} = D_{\text{M}} = D_{\text{Ryd}} \tag{13}$$

and

$$a^2 = 2\alpha^2 R^2 = 72, \tag{14}$$

respectively. The relationship described in equation (14) can also be obtained by comparing terms in equation (11). Hence equations (11)–(14) provide a simultaneous connection, for near equilibrium, among the four classical potentials considered herein.

To obtain a long range relationship, there is a need to compare the coefficients and the indices of the repulsive and attractive terms of the potentials. The Rydberg potential in the original form, equation (3), does not give any clear distinction between the repulsive and attractive terms. To pave a way for comparison, equation (3) is rewritten in the form

$$U_{\text{Ryd}} = D_{\text{Ryd}} \left[a \left(1 - \frac{r}{R}\right) - 1 \right] \exp\left(a \left(1 - \frac{r}{R}\right)\right) \tag{15}$$

and, upon recalling the Maclaurin series expansion for the following exponential function

$$\exp\left[a \left(1 - \frac{r}{R}\right)\right] = 1 + \frac{a \left(1 - r/R\right)}{1!} + \frac{a^2 \left(1 - r/R\right)^2}{2!} + \cdots , \tag{16}$$

we substitute the approximation

$$a \left(1 - \frac{r}{R}\right) \approx \exp\left[a \left(1 - \frac{r}{R}\right)\right] - 1 \tag{17}$$

into the square parenthesis of equation (15) to yield

$$U_{\text{Ryd}} \approx D_{\text{Ryd}} \left[\exp\left(2a \left(1 - \frac{r}{R}\right)\right) - 2\exp\left(a \left(1 - \frac{r}{R}\right)\right)\right]. \tag{18}$$

Likewise, the Morse potential can be rewritten in such a manner to enable comparison of its indices as follows

$$U_{\text{M}} = D_{\text{M}} \left[\exp\left(2\alpha R \left(1 - \frac{r}{R}\right)\right) - 2\exp\left(\alpha R \left(1 - \frac{r}{R}\right)\right)\right]. \tag{19}$$

Therefore, comparing the coefficients and indices of both the repulsive and attractive terms of equations (1), (12), (18) and (19), we observe the following connection

$$\xi = 12 = 2\alpha R = 2a \tag{20}$$

for long range. The justification for comparing coefficients and indices of the term containing $\exp(1 - r/R)$ with those containing (R/r) is on the basis the Maclaurin series expansions

$$\exp\left(1 - \frac{r}{R}\right) = 1 - \frac{(\delta r/R)^1}{1!} + \frac{(\delta r/R)^2}{2!} - \cdots \tag{21}$$

and

$$\frac{R}{r} \equiv \frac{1}{1 - (-\delta r/R)} = 1 - \left(\frac{\delta r}{R}\right)^1 + \left(\frac{\delta r}{R}\right)^2 - \cdots, \tag{22}$$

which allows for the approximation

$$\exp\left(1 - \frac{r}{R}\right) \approx \frac{R}{r} \approx 1 - \frac{\delta r}{R} \tag{23}$$

for $|\delta r/R| < 1$ whereby $\delta r = r - R$.

To relate the modern potentials to the classical ones, we observe that the 2-body portion of the BMS potential

$$U_{\text{BMS}} = A \exp\left(-Br\right) - \frac{C}{r^n} \tag{24}$$

coincides exactly with Bucking potential for the case where $n = 6$. To relate the Morse potential and the 2-body portion of the BH potential

$$U_{\text{BH}} = A_1 \exp\left(-\lambda_1 r\right) + A_2 \exp\left(-\lambda_2 r\right), \tag{25}$$

we set

$$\left(\frac{\partial U_{\mathrm{BH}}}{\partial r}\right)_{r=R} = 0 \tag{26}$$

to obtain

$$\lambda_1 A_1 \exp\left(-\lambda_1 R\right) = -\lambda_2 A_2 \exp\left(-\lambda_2 R\right) \tag{27}$$

so that equation (25) can be rewritten as

$$U_{\mathrm{BH}} = A_1 \exp\left(-\lambda_1 R\right) \left[\exp\left(-\lambda_1(r-R)\right) - \frac{\lambda_1}{\lambda_2}\exp\left(-\lambda_2(r-R)\right)\right]. \tag{28}$$

In this way, comparison between equations (2) and (28) suggests

$$\left\{\begin{matrix} \lambda_1 \\ \lambda_2 \end{matrix}\right\} = \alpha \left\{\begin{matrix} 2 \\ 1 \end{matrix}\right\} \tag{29}$$

and

$$D_{\mathrm{M}} = A_1 \exp\left(-\lambda_1 R\right), \tag{30}$$

where R is obtainable from equation (27).

The entire simultaneous connections amongst the four classical pair potentials, and their relations to 2-body portions of modern many-body potentials, are summarized in table 2.

Table 2
Parametric connections among the considered interatomic potential functions.

Potential functions	Parametric connections
Among the four classical potentials	$D_{\mathrm{LJ}} = D_{\mathrm{M}} = D_{\mathrm{Ryd}} = \left(\frac{\xi-6}{6}\right) A \exp\left(-\xi\right) = \left(\frac{\xi-6}{\xi}\right)\left(\frac{B}{\xi}\right)^6 C$
$U_{\mathrm{LJ}} = U_{\mathrm{LJ}}(D_{\mathrm{LJ}}, R, r)$	For near-equilibrium,
$U_{\mathrm{M}} = U_{\mathrm{M}}(D_{\mathrm{M}}, \alpha, R, r)$	$\xi = RB = \left(\frac{7}{2}+\frac{S^2}{6}\right) + \sqrt{\left(\frac{7}{2}+\frac{S^2}{6}\right)^2 - 2S^2}$
$U_{\mathrm{Ryd}} = U_{\mathrm{Ryd}}(D_{\mathrm{Ryd}}, a, R, r)$	where $S = 6 = \alpha R = \frac{a}{\sqrt{2}}$.
$U_{\mathrm{B}} = U_{\mathrm{B}}(A, B, C, r)$	For long-range, $\frac{\xi}{2} = 6 = \alpha R = a$.
Between Morse and 2-body portion of	$D_{\mathrm{M}} = A_1 \exp\left(-\lambda_1 R\right) = -\frac{\lambda_2}{\lambda_1} A_2 \exp\left(-\lambda_2 R\right)$
BH potentials	
$U_{\mathrm{M}} = U_{\mathrm{M}}(D_{\mathrm{M}}, \alpha, R, r)$	$\alpha = \frac{\lambda_1}{2} = \lambda_2$
$U_{\mathrm{BH}} = U_{\mathrm{BH}}(A_1, A_2, \lambda_1, \lambda_2, r)$	$R = \frac{1}{\lambda_1 - \lambda_2}\ln\left(-\frac{\lambda_1 A_1}{\lambda_2 A_2}\right)$
Between Buckingham and the 2-body	
portion of BMS	
$U_{\mathrm{B}} = U_{\mathrm{B}}(A, B, C, r)$	$n = 6$
$U_{\mathrm{BMS}} = U_{\mathrm{BMS}}(A, B, C, n, r)$	

3.   Results and discussion

Verification can be made by observing theoretical plots of non-dimensional interatomic potential energy (U/D) against the non-dimensional interatomic distance (r/R). Applying the near-equilibrium relationships and the long range relationships, as furnished in table 2, into the classical potentials described in equations (1)–(3) and (12), we have the curves of (U/D) versus (r/R), as shown in figures 2 and 3 for near-equilibrium and long range, respectively. Whilst the magnitude of D quantifies the bond strength (high D for strong bonds, low D
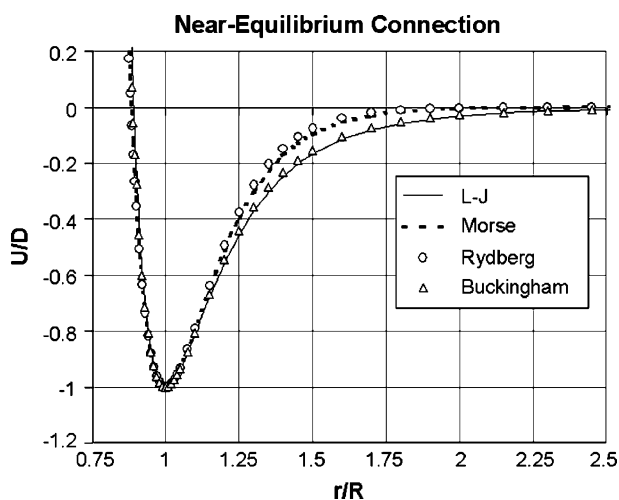

Figure 2. Plots of the four classical potentials simultaneously connected for near-equilibrium.
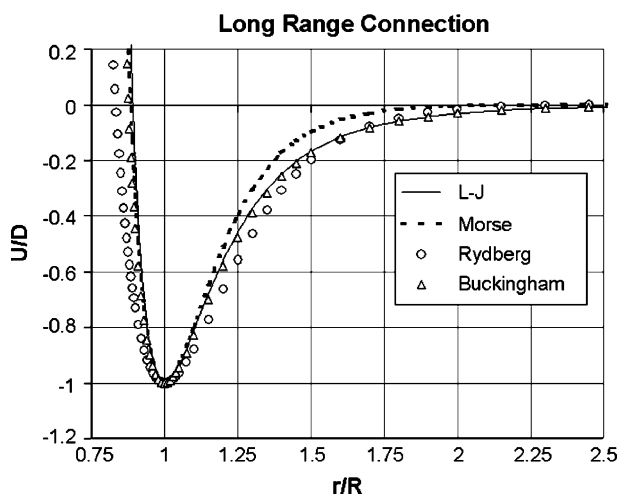

Figure 3. Plots of the four classical potentials simultaneously connected for long-range.

for weak bonds), the shape of (U/D) versus (r/R) describes how "hard" or how "soft" the bond is, regardless of the bond strength. An acute rise in (U/D) versus (r/R) followed by a more abrupt leveling-off indicates the bond hardness that characterizes a covalent-type (or hard, solid-like) bond, whilst a gradual rise in (U/D) versus (r/R) signifies a van der Waals-type (soft, fluid-like) bond. This can be inferred from the fact that the interatomic force is related to the potential energy and interatomic separation distance as

$$F = -\frac{\partial U}{\partial r}, \tag{31}$$

thereby denoting a sharp drop in interatomic force during interatomic separation of "hard" bonds. As such, imposition of equal derivatives of the potential energy up to the second order at $r = R$ not only gives equal curvature there (see figure 2), but also reveals the shape of (U/D) versus (r/R). It is therefore of no surprise that the Lennard-Jones and the Buckingham potentials are normally employed in computational chemistry softwares for describing van der Waals interaction, while Morse and Rydberg (2-body MM) potentials are used for covalent bonds in molecules and in solid-state matter.

In the case of parametric relationship for long range, relaxing the imposition of equal second order derivative at $r = R$ no longer results in equal curvature there. However the sacrifice of equal curvature at equilibrium enables good agreement to be made for $r > R$. This is especially observed for the case of Rydberg curve whereby a decrease in curvature at equilibrium enables an overall drop in the potential energy, thereby allowing reasonable correlation with the Lennard-Jones and the Buckingham potentials for long range.

Connection between the Morse and 2-body BH as well as that between Buckingham and 2-body BMS are not plotted due to their exact relationship shown in table 2.

4.   Conclusions

A relationship between the four classical interatomic pair potentials has been developed in this paper, thereby establishing their simultaneous connections. This was done by imposing equal potential energy, and their first two derivatives at equilibrium as well as the usage of calculus and Maclaurin series expansions. Discrepancies were shown via theoretical plots of (U/D) versus (r/R), thereby elucidating the choice of potential functions used for quantifying different types of interatomic interaction in computational chemistry and solid-state softwares.

References

[1] J.E. Lennard-Jones, Proc. Roy. Soc. Lond. A 106 (1924) 463.

 [2] P.M. Morse, Phys. Rev. 34 (1929) 57.
 [3] R. Rydberg, Z. Phys. 73 (1931) 376.
 [4] R.A. Buckingham, Proc. Roy. Soc. Lond. A 168 (1938) 264.
 [5] E. Pearson, T. Takai, T. Halicioglu and W.A. Tiller, J. Cryst. Growth 70 (1984) 33.
 [6] R. Biswas and D.R. Hamann, Phys. Rev. Lett. 55 (1985) 2001.
 [7] J.N. Murrell and R.E. Mottram, Mol. Phys. 69 (1990) 571.
 [8] R. Bauer, W. Maysenholder and A. Seeger, Phys. Lett. A 90 (1982) 55.
 [9] T.C. Lim, J. Math. Chem. 31 (2002) 421.
[10] T.C. Lim, J. Math. Chem. 32 (2002) 249.
[11] T.C. Lim, J. Math. Chem. 33 (2003) 29.
[12] T.C. Lim, J. Math. Chem. 33 (2003) 279.
[13] T.C. Lim, MATCH Commun. Math. Comput. Chem. 49 (2003) 155.
[14] T.C. Lim, J. Math. Chem. 34 (2003) 221.
[15] T.C. Lim, Z. Naturforsch. A 58 (2003) 615.
[16] T.C. Lim, MATCH Commun. Math. Comput. Chem. 50 (2004) 185.
[17] T.C. Lim, Z. Naturforsch. A 59 (2004) 116.
[18] T.C. Lim, Czech. J. Phys. 54 (2004) 553.
[19] T.C. Lim, J. Math. Chem. 36 (2004) 139.
[20] T.C. Lim, J. Math. Chem. 36 (2004) 147.